J. Fluid Mech. (2003), *vol.* 486, *pp.* 105–114.
DOI: 10.1017/S0022112003004270 Printed in the United Kingdom

On geometry effects in Rayleigh–Bénard convection

By SIEGFRIED GROSSMANN[1] AND DETLEF LOHSE[2]

[1]Department of Physics, University of Marburg, Renthof 6, D-35032 Marburg, Germany

[2]Department of Applied Physics and J. M. Burgers Centre for Fluid Dynamics
University of Twente, P.O. Box 217, 7500 AE Enschede, The Netherlands

(Received 3 January 2003 and in revised form 21 February 2003)

Various recent experiments hint at a geometry dependence of scaling relations in Rayleigh–Bénard convection. Aspect ratio and shape dependences have been found. In this paper a mechanism is suggested which can account for such dependences, based on Prandtl's theory for laminar boundary layers and on the conservation of volume flux of the large-scale wind. The mechanism implies the possibility of different thicknesses of the kinetic boundary layers at the sidewalls and at the top/bottom plates, as found experimentally, and also different Ra-scaling of the wind over the plates and at the sidewalls. A scaling argument for the velocity and temperature fluctuations in the bulk is also developed.

1. Introduction

Turbulent Rayleigh–Bénard convection is one of the classical problems in fluid dynamics, see e.g. Siggia (1994), Kadanoff (2001), Ahlers, Grossmann & Lohse (2002). The great interest in this problem also originates from the relevance of thermal turbulence to meteorology, geophysics, oceanography, and astrophysics. However, unlike these flows in nature, in laboratory experiments the thermal convection is confined to a container. Because of the confinement, boundary layers (BL) play a prominent role. This is the case for both the thermal and the kinetic BLs and for both the top/bottom and the sidewall BLs.

While it is obvious that the thermal BLs at the (heated or cooled) plates and at the (thermally isolated) sidewalls are different in nature from each other, unexpectedly the kinetic BLs at the plates and at the sidewalls not only have different thicknesses, but even scale differently: Qiu & Xia (1998*a*) and Lam *et al.* (2002) found that these velocity BL thicknesses (which are set by the mean flow velocity profile above the wall) scale with Rayleigh number Ra and Prandtl number Pr as $\delta_w/L = 3.6\ Ra^{-0.26\pm0.03}$ at the sidewalls and as $\delta_p/L = 0.65\ Ra^{-0.16\pm0.02}\ Pr^{0.24\pm0.01}$ at the top or bottom plates, both measured in an aspect ratio $\Gamma = 1$ cylindrical cell. Moreover, Qiu & Tong (2001) find different mean velocity amplitudes (not different Ra-scaling) at the sidewalls and at the plates, $U_w \neq U_p$. The notation is summarized in figure 1.

No existing theory of Rayleigh–Bénard convection accounts for these differences in the BL thicknesses or the flow velocities. The unifying theory of thermal convection of Grossmann & Lohse (2000, 2001, 2002) allows only for one kinetic boundary layer thickness, and gives an effective power-law exponent -0.22 (for $\Gamma = 1$ and $Pr = 6$) (Grossmann & Lohse 2002), close to the average $(-0.16 - 0.26)/2 = -0.21$ of the experimental results for the plate and the wall BLs thicknesses. The mechanisms

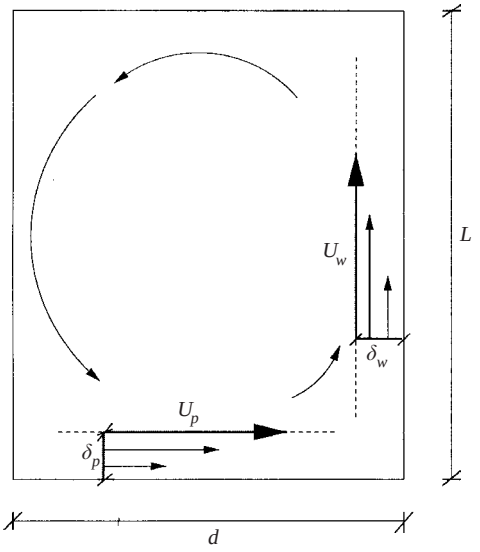

FIGURE 1. Notation for the plate and sidewall BLs. The cell is cylindrical and heated from below and cooled from above. Subscript p denotes variables at the top and bottom plates, and w those at the sidewalls. The large-scale wind is sketched.

suggested in the present paper to deal with the observed BL differences are independent of our recent unifying theory (Grossmann & Lohse 2000, 2001, 2002). However, that unifying theory can be extended to reflect the differences between the sidewall and plate BLs, as sketched in the Appendix.

The different BL thicknesses and velocities near the sidewalls and the top/bottom plates lead to an aspect-ratio dependence of various quantities. Xu, Bajaj & Ahlers (2000), Ahlers & Xu (2001) and Qiu & Tong (2001) find in experiments with cylindrical cells that the prefactors of the effective *Nu* versus *Ra* power laws depend on the aspect ratio. Also Niemela & Sreenivasan (2003) find an aspect ratio dependence of the heat flow at large *Ra*, and conclude that the focus of the next generation of experiments must be on large-aspect-ratio cells. Daya & Ecke (2001) find that the bulk temperature and velocity fluctuations in a cylindrical cell and in a square cell are very different, again an indication that the geometrical details of the container are important and measurable.

In this paper we set out to suggest a physical mechanism to account for the difference between the wall and plate velocity field BLs and for the aspect ratio and shape dependence in Rayleigh–Bénard convection. We restrict ourselves to a cylindrical cell with an aspect ratio about 1. The starting point is Prandtl's BL theory. The main physical ingredient is the conservation of the volume flux of the large-scale wind (§ 2). The main results (§ 3) are (3.4*a*) and (3.4*b*), the ratios of the wall and plate BL thicknesses and the wall and plate velocities, which now both have a Reynolds and thus Rayleigh number dependence. We hope these equations capture the physical mechanism to account for the different behaviour of the sidewall and plate BLs (§ 3) and for the aspect ratio dependences (§ 4). In § 5 we present scaling arguments for the fluctuations of the velocity and the temperature in the bulk. These were not included in the unifying theory of Grossmann & Lohse (2000, 2001, 2002). We do this here, because the bulk fluctuations also seem to show geometry effects, cf. Daya & Ecke (2001).

2. Implications of Prandtl–Blasius theory for laminar boundary layers

Laminar BL flow is described by the well-known Prandtl equations (Prandtl 1904; Blasius 1908; Landau & Lifshitz 1987). The BL thickness is not constant over the plates or the walls, see Qiu & Xia (1998*b*). The values of δ_p or δ_w should be understood as typical thicknesses at the centre of the plates or at half-height, respectively. In the equations streamwise lengths are scaled by the streamwise length scale l, while wall-normal lengths are (re)scaled by $l/\sqrt{Re}$. Here, $Re = lU_0/\nu$ is the Reynolds number based on l and the streamwise velocity scale U_0. Correspondingly, streamwise velocities are scaled by U_0 and wall-normal velocities by $U_0/\sqrt{Re}$. The immediate consequence is that the thickness of the laminar BL scales as $\delta \sim l/\sqrt{Re}$; see e.g. Landau & Lifshitz (1987, section 39).

In the context of Rayleigh–Bénard convection this means that the relevant streamwise length scales are the width d of the cell for the plates and the height L of the cell for the walls, i.e. different for cells with non-unity aspect ratio $\Gamma = d/L$. Correspondingly, according to the Prandtl theory, the widths of the velocity field BLs at the walls and at the plates are also different, namely

$$\delta_w = a\frac{L}{\sqrt{U_w L/\nu}}, \quad \delta_p = a\frac{d}{\sqrt{U_p d/\nu}}, \tag{2.1a,b}$$

respectively. Here, a is a dimensionless prefactor of order 1; Blasius (1908) gave $a = 1.72$ for a semi-infinite kinetic BL, cf. also Landau & Lifshitz (1987)†.

The naive assumption now would be that the streamwise wall and plate velocities are the same, $U_w = U_p$. The immediate consequence would be aspect-ratio-dependent BL widths $\delta_w = \delta_p/\sqrt{\Gamma}$, but (i) δ_w and δ_p would still show the same Reynolds and therefore Rayleigh number scaling and (ii) the experiments by Qiu & Tong (2001) have shown that the assumption $U_w = U_p$ does not hold.

Therefore, we must find a more realistic argument. Our suggestion is that volume flux conservation is an appropriate (and weak) starting assumption, i.e. we assume equal volume fluxes of the wind over the walls and the plates,

$$\dot{V}_w = \dot{V}_p. \tag{2.2}$$

We consider volume flux conservation to be an expression of incompressibility. To proceed further, we must examine the flow geometry more closely.

3. Laterally restricted vs. plate filling flow

The flow geometry is only roughly known, e.g. from flow visualizations (Tong-group) or from numerical simulations (Verzicco & Camussi 1999, 2003; Verzicco 2002). For a cylindrical cell with an aspect ratio of about 1 (say $1/2 < \Gamma < 2$), to which we restrict ourselves here, one large convection roll seems to exist.‡ How does this roll flow over the plates? We shall discuss two extremes, which we denote as the 'laterally restricted' flow, and the 'plate filling' flow, see figure 2. The flow is called laterally restricted if the convection roll has the same spanwise extent both at the

† For large enough Rayleigh number the laminar BL will become turbulent and then the theory presented here must be modified. Both Grossmann & Lohse (2002) and Niemela & Sreenivasan (2003*a*) expect the transition towards a turbulent BL to occur around $Ra \sim 10^{14}$ (for $Pr \sim 1$).

‡ In a square box the flow pattern can be very complicated, including region of backflow and secondary flows, see e.g. figure 1 of Qiu & Xia (1998*b*). These geometrical complications are the reason why we restrict consideration to flow in a cylindrical box with an aspect ratio of about 1.

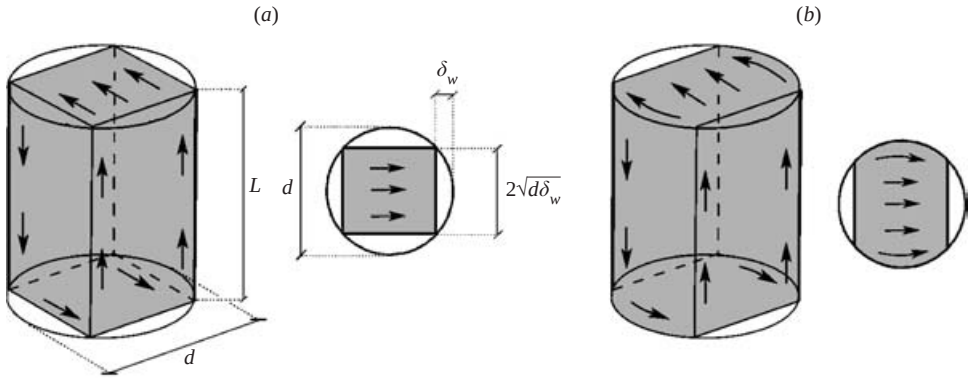

FIGURE 2. (a) Laterally restricted and (b) plate filling flow in a cylindrical cell. For each, the left-hand drawings show sketches of the three-dimensional flow, the right-hand ones a top view on the bottom plate. The flow area above the plate is shaded. The spanwise extent of the wind along the walls is $2\sqrt{d\delta_w}$ and follows from trigonometry for given layer width δ_w and cylinder radius $d/2$.

plates and the walls. In contrast, the flow is said to be plate filling if it covers the full plate width d in the middle, whereas towards the walls its extent is only $2\sqrt{d\delta_w}$. Physically this smaller spanwise size of the BL at the wall expresses the idea that for a wall layer of width δ_w above a curved wall with radius of curvature $d/2$ the layer's lateral extent is automatically restricted. Mathematically this follows from applying Pythagoras' theorem, see figure 2(a), right, valid for small $\delta_w \ll d$. The real flow will be between these two extremes, but in order to reveal the mechanism, we shall restrict ourselves to these well-defined extremes. The different physics of these extreme situations is obvious from figures 2(a) and 2(b): in the plate filling case the flow over the plate has more spanwise extent. Due to mass flow conservation, the flow velocity over the plate therefore can be smaller and according to Prandtl's theory (2.1b) the plate BL thickness is larger than for the laterally restricted case.

Laterally restricted flow: The spanwise length scale of the flow is $2\sqrt{d\delta_w}$ at the walls and at the plates (see figure 2a). The corresponding volume fluxes are $\dot{V}_w = 2\sqrt{d\delta_w}\delta_w U_w$ at the walls and $\dot{V}_p = 2\sqrt{d\delta_w}\delta_p U_p$ at the plates. With volume flux conservation (2.2) and the Prandtl relations (2.1a, b) we immediately obtain

$$\delta_w/\delta_p = \Gamma^{-1}, \quad U_p/U_w = \Gamma^{-1}. \tag{3.1a,b}$$

Thus the wall and plate BLs have different thicknesses and velocities. But there is no difference in the Ra-scaling of δ_w and δ_p, in contrast to what was found by Qiu & Xia (1998a). The ratio of the boundary layer Reynolds numbers $Re_{\delta_w} = U_w\delta_w/\nu$ and $Re_{\delta_p} = U_p\delta_p/\nu$ is

$$Re_{\delta_w}/Re_{\delta_p} = 1. \tag{3.1c}$$

Plate filling flow: The spanwise length scale of the flow at the cylindrical walls still is $2\sqrt{d\delta_w}$. But now by definition the flow over the plates is extended spanwise to fully cover the plate area, laterally of order d. The corresponding volume fluxes are now $\dot{V}_w = 2\sqrt{d\delta_w}\delta_w U_w$ at the wall, as before, but $\dot{V}_p = d\delta_p U_p$ at the plate. Using again volume flux conservation (2.2) and the Prandtl relations (2.1a, b) we now obtain $U_p^2/U_w = \nu L^{-1}\Gamma^{-4}2^4a^4$ and

$$\delta_w/\delta_p = \Gamma^{-1/2}\sqrt{U_p/U_w}\ . \tag{3.2}$$

For convenience we nondimensionalize the wall and the plate wind velocities with the same molecular velocity ν/L and introduce the wall and plate Reynolds numbers,

$$Re_w = U_w L/\nu, \qquad Re_p = U_p L/\nu. \tag{3.3}$$

Note that both are defined with the height L of the cell. With these definitions we find

$$\delta_w/\delta_p = \Gamma^{-5/2} 4a Re_p^{-1/2} = \sqrt{4a}\,\Gamma^{-3/2} Re_w^{-1/4}, \tag{3.4a}$$

$$U_p/U_w = Re_p/Re_w = \Gamma^{-4} 16a^2 Re_p^{-1} = 4a\Gamma^{-2} Re_w^{-1/2}, \tag{3.4b}$$

$$Re_{\delta_w}/Re_{\delta_p} = (4a)^{-1}\Gamma^{3/2} Re_p^{1/2} = (4a)^{-1/2}\Gamma^{1/2} Re_w^{1/4}. \tag{3.4c}$$

Equations (3.4*a*) and (3.4*b*) are our main results. They show, for plate filling flow, a Reynolds number and thus a Rayleigh number dependence of the ratio between the BL thicknesses at the wall and at the plate, due to the cylindrical shape of the container; δ_w and δ_p scale differently with Ra, as experimentally observed by Qiu & Xia (1998*a*). The physics of the mechanism is that the extent of the flow (fully covering the plates in the assumed extreme case) allows a larger flow cross-section, which slows down the plate velocity U_p. Due to Prandtl's theory (2.1*b*) this means a thicker BL above the plates. Equation (3.4*c*) means that the BL Reynolds number at the wall grows faster (with Ra) than at the plates, implying that the first instability of the BLs towards turbulence should occur at the sidewalls, not at the plates – a prediction which is directly testable.

Since experimental flows are expected to lie in between the laterally restricted and the plate filling cases, δ_w/δ_p should be between $Re_p^{-1/2}$ and Re_p^0 or between $Ra^{-0.22}$ and Ra^0; here we have used the effective scaling $Re_p \sim Ra^{0.45}$ which holds for $Pr = 5$ and $\Gamma = 1$ both experimentally (Qiu & Tong 2001, who measure the *plate* Reynolds number Re_p which they call Re_γ, extracted from the slope of the (linear) profile of the horizontal velocity above the bottom plate.) and theoretically (Grossmann & Lohse 2002) for $10^8 < Ra < 10^{10}$. The experimental ratio has a scaling exponent in between the values given by the plate filling and the laterally restricted cases, namely $\delta_w/\delta_p \sim Ra^{-0.11}$ (Qiu & Xia 1998). That the exponent is just the arithmetic mean is presumably just incidental. Note however that the cell in the experiments by Qiu & Xia (1998*b*) is a square box, and not a cylinder as here, and, in those square box experiments no Rayleigh number dependence of the *velocity* ratio U_p/U_w is found – though the ratio is clearly different from unity.

4. Aspect-ratio dependences

We now come to the aspect ratio dependence of δ_w/δ_p and U_p/U_w. For $\Gamma = 1/2$ and $\Gamma = 2$ these ratios (normalized to $\Gamma = 1$) are summarized in table 1. The experimental data are obtained from figure 3 ($\Gamma = 1$, $Ra = 3.7 \times 10^9$), figure 6 ($\Gamma = 2$, $Ra = 4.9 \times 10^8$), and figure 8 ($\Gamma = 1/2$, $Ra = 3.28 \times 10^{10}$) of Qiu & Tong (2001). In these figures both Γ and Ra were changed at the same time. In order to compare the ratios at $\Gamma = 2$ measured at $Ra = 5 \times 10^8$ with those at $\Gamma = 1$ measured at $Ra = 3.7 \times 10^9$, they first have to be extrapolated to this higher Ra. Correspondingly, in the $\Gamma = 1/2$ case we have to extrapolate the ratios from the original value $Ra = 3.3 \times 10^{10}$ to $Ra = 3.7 \times 10^9$. These extrapolations have been done according to the plate filling case formulas (3.4*a*, *b*) or according to the laterally restricted case ones (3.1*a*, *b*). In

	Model	$\Gamma = 1$	$\Gamma = 1/2$	$\Gamma = 2$
δ_w/δ_p	exp., extrapol: laterally restricted	1	2.1	0.29
	exp., extrapol: plate filling	1	3.3	0.19
	theory, laterally restricted	1	2.0	0.50
	theory, plate filling	1	5.6	0.18
U_p/U_w	exp., extrapol: laterally restricted	1	1.2	2.0
	exp., extrapol: plate filling	1	3.1	0.8
	theory, laterally restricted	1	2.0	0.5
	theory, plate filling	1	16	0.063

TABLE 1. δ_w/δ_p and $U_p/U_w = Re_p/Re_w$ for different aspect ratios, normalized to $\Gamma = 1$, where we have put these ratios to 1. The Reynolds number $Re_p = 3.7 \times 10^9$ is fixed and the experimental values are extrapolated to that Re_p, see text. Note that the error in reading off in particular the boundary layer widths from the figures 3, 6, and 8 of Qiu & Tong (2001) is at least 25% and therefore the experimental ratios should only be taken as a very rough estimate.

the latter case no extrapolation is necessary as in those equations there is no Ra or Re dependence. We always suppose that there is one-roll state for all Γ.

From table 1 we conclude that the experimental results (if extrapolated with the plate filling flow model) in general lie in between the predictions of the laterally restricted and plate filling cases, just as expected. An exception is U_p/U_w for $\Gamma = 2$; we have no explanation for that. If extrapolated with the laterally restricted flow model the velocity ratios for neither $\Gamma = 1/2$ nor $\Gamma = 2$ lie between the predictions of the two flow cases.

The physics of the aspect-ratio dependence is as follows. For increasing aspect ratio the available plate area of the flow increases and the plate velocity can decrease. According to the Prandtl law (2.1*b*), the plate BL thickness then increases. At the walls there is no additional lateral space for larger aspect ratios, therefore the flow has to accelerate, $U_w > U_p$, and correspondingly $\delta_w < \delta_p$.

Note that the above dependence on Γ was derived assuming there is one convection roll. Once the convection develops two rolls on top of each other (for Γ less than 1) or next to each other (for Γ larger than 1), the aspect ratio dependence has to be considered in a more sophisticated way. For small $\Gamma \leqslant 1/2$ a transition from one roll to two rolls has been observed numerically by Werne (1993) and Verzicco & Camussi (2003). In experiments both states of convection have also possibly been realized, see the discussion in Niemela & Sreenivasan (2003). Thus one cannot formally consider $\Gamma \to 0$ or $\Gamma \to \infty$ in (3.1)–(3.4) without checking the proviso for their validity that precisely one convection roll is obtained.

Can one manipulate a system such that it is no longer between the laterally restricted and the plate filling cases? An option may be to take a square box and slightly tilt it in order to disfavour the flow along the diagonal, which seems to occur without tilting (Daya & Ecke 2001). Such tilting experiments have successfully been done by Ciliberto, Cioni & Laroche (1996). Such flow is expected to follow the laterally restricted flow model with confinement by the left and right walls. For this type of flow (3.1*a*) should hold, i.e. the wall and the plate BLs should show the same Ra-scaling. An experimental test of this prediction seems a worthwhile check on the proposed theory.

5. Scaling relations for bulk velocity and temperature fluctuations

Up to now we have dealt with the BLs. Since experiments, cf. Daya & Ecke (2001), show that the bulk velocity and temperature fluctuations u' and θ' also seem to depend on the geometry, we should consider these too. Experiments, see e.g. Castaing *et al.* (1989) and Lam *et al.* (2002), suggest that u' scales differently from the large-scale velocity U, namely with a weaker Ra dependence. Typically, the fluctuation Reynolds number is $Re' = u'L/\nu \sim Ra^{0.40\pm0.03}$ while the large-scale velocity Reynolds number is $Re = UL/\nu \sim Ra^{0.43\ldots0.50}$ (Castaing *et al.* 1989; Niemela *et al.* 2001; Lam *et al.* 2002; Siggia 1994; Qiu & Tong 2001). In previous discussions Re_w and Re_p have not yet been distinguished. We therefore understand Re to be an unknown average of them. In Grossmann & Lohse (2000, 2001, 2002) we developed a theory for the dependences of the large-scale quantities $Re(Ra, Pr)$ and $Nu(Ra, Pr)$ on Ra and Pr. Here we add the argument that the bulk fluctuations Re' and θ' should behave as functions of Ra and Pr.

The turbulence in the bulk is driven by the large-scale wind; therefore the energy dissipation rate in the bulk $\epsilon_{u,b}$ scales as $\epsilon_{u,b} \sim U^3/L$ as in Grossmann & Lohse (2000, 2001, 2002). The energy cascades down and will be dissipated on scales comparable to the Kolmogorov scale $\eta = (\nu^3/\epsilon_{u,b})^{1/4}$. Thus we can estimate the bulk dissipation also by $\epsilon_{u,b} \sim \nu u'^2/\eta^2$. Relating u' with U yields

$$Re' \sim Re^{3/4}. \tag{5.1}$$

With $Re \sim Ra^{0.43\ldots0.50}$ this means $Re' \sim Ra^{0.32\ldots0.38}$, which is close to the experimental finding $Re' \sim Ra^{0.40\pm0.03}$ by Lam *et al.* (2002) and also to the finding by Daya & Ecke (2001) $Re' \sim Ra^{0.36\pm0.05}$ for a square cell.

The same reasoning can be followed to calculate the scaling of the typical bulk temperature fluctuations θ'. The thermal bulk dissipation is driven by the large-scale temperature Δ; its time scale again is taken as L/U. Thus the thermal dissipation rate in the bulk scales as $\epsilon_{\theta,b} \sim \Delta^2 U/L$. On the other hand, the thermal energy in the bulk is dissipated by the temperature fluctuations θ' on scale $\eta_\theta = (\kappa^3/\epsilon_{u,b})^{1/4} \sim LPr^{-3/4}Re^{-3/4}$, according to $\epsilon_{\theta,b} \sim \kappa\theta'^2/\eta_\theta^2$. Thus

$$\theta'/\Delta \sim Pr^{-1/4}Re^{-1/4}\ . \tag{5.2}$$

Experimentally Lam *et al.* (2002) measured $Re \sim Ra^{0.43}\ Pr^{-0.76}$, which holds for $10^8 < Ra < 3\times10^{10}$ and $3 < Pr < 1200$. This means $\theta'/\Delta \sim Pr^{-0.06}\ Ra^{-0.11}$. For $Re \sim Ra^{1/2}$ (Castaing *et al.* 1989; Niemela *et al.* 2001) one obtains $\theta'/\Delta \sim Ra^{-0.13}$. Both power laws are very close to the experimental findings $\theta'/\Delta \sim Ra^{-1/7}$ (Castaing *et al.* 1989) or $\theta'/\Delta \sim Ra^{-0.10\pm0.02}$ (Daya & Ecke 2001) for cylindrical cells.

6. Conclusions

We have suggested a possible mechanism to qualitatively understand the different Ra behaviours of the kinetic BLs near the plates and the sidewalls and the recently observed effects of the Rayleigh–Bénard cell geometry. Our picture has yet to be confirmed in more experimental detail. In particular, the comparison of Rayleigh–Bénard convection in a square cell with diagonal (plate filling case) and with edge parallel (laterally restricted case) wind seems promising. Another problem is to distinguish the one-roll from the two-roll (or more) states. Also the exact orientation of the roll in the cylindrical cell is relevant and needs attention: Niemela & Sreenivasan (2003*b*) speculate that for lower Ra it takes an elliptical form, whereas it becomes increasingly squarer for larger Ra.

In any case, measuring the large-scale wind velocity should take into consideration that possibly $U_p \neq U_w$. Circulation time measurements average over both, while local methods can distinguish U_p and U_w. An obvious first experimental step to gain insight into whether the suggested mechanism is correct would be to directly measure the ratios U_p/U_w and δ_p/δ_w as a function of aspect ratio, exact position in the cell, and Reynolds number; for both ratios we have offered qualitative predictions, namely that they lie between our results for the laterally restricted and the plate filling cases. Finally, we have indicated how the different scalings of bulk fluctuations and large-scale quantities are related.

We thank X. van Doornum for drawing figure 2. The work is part of the research program of FOM, financially supported by NWO. It was also supported by the European Union (EU) under contract HPRN-CT-2000-00162 and by the German-Israeli Foundation (GIF).

Appendix. Kinetic and thermal dissipation in the BLs

Within the framework of the present paper, the different behaviours of the sidewall and plate BLs and their aspect-ratio dependences can also be included into the unifying theory of thermal convection by Grossmann & Lohse (2000, 2001, 2002). The main idea of that theory is to split the velocity field dissipation rate ϵ_u and the thermal dissipation rate ϵ_θ, for which exact global relations can be derived from the Boussinesq equations, into their bulk and BL contributions.

For the kinetic dissipation this splitting obviously can be extended to

$$\epsilon_u = \epsilon_{u,p} + \epsilon_{u,w} + \epsilon_{u,b}, \tag{A 1}$$

where $\epsilon_{u,p}$, $\epsilon_{u,w}$ denote the kinetic dissipation rates in the plate or wall BLs, and $\epsilon_{u,b}$ the bulk kinetic dissipation rate. Following Grossmann & Lohse (2000), the BL dissipations are estimated as

$$\epsilon_{u,p} = \nu \frac{U_p^2}{\delta_p^2}\frac{\delta_p}{L} = \frac{\nu^3}{L^4}\frac{1}{a\Gamma^{1/2}} Re_p^{5/2} = \frac{\nu^3}{L^4} 2^5 a^{3/2}\Gamma^{-9/2} Re_w^{5/4}, \tag{A 2}$$

$$\epsilon_{u,w} = \nu \frac{U_w^2}{\delta_w^2}\frac{\delta_w}{l} = \frac{\nu^3}{L^4}\frac{\Gamma^9}{2^{10}a^6} Re_p^5 = \frac{\nu^3}{L^4}\frac{1}{a\Gamma} Re_w^{5/2}. \tag{A 3}$$

The bulk dissipation rate $\epsilon_{u,b}$ has already been dealt with in § 5.

For the thermal dissipation rate the partition into BLs and bulk contributions is different. Though in ideal Rayleigh–Bénard convection the sidewalls are perfectly isolated (no-flux condition), thermal BLs can develop at the sidewalls, as observed both in numerical simulations and in experiment (Ahlers 2000; Ching & Lo 2001; Ching & Pang 2002; Verzicco & Camussi 2003; Verzicco 2002; Qiu & Tong 2001). However, within the unifying theory of Grossmann & Lohse (2000, 2001, 2002) the sidewall and bulk thermal dissipation rates are not separated. Instead, we introduce the notation $\epsilon_{\theta,p}$ for the thermal dissipation rates in the BLs near the top and bottom plates and $\epsilon_{\theta,\bar{p}}$ for the thermal dissipation elsewhere, i.e. within the bulk and within the sidewall BLs ($\bar{p}$ indicates 'non-plate').

The physical reason for the different treatment of the top and bottom thermal BLs and the sidewall thermal BLs originates from the exact relation $\epsilon_\theta = \kappa\Delta^2 L^{-2} Nu$. Now, Nu is the temperature flux density from bottom to top. This flux is a vector perpendicular to the top/bottom plates but parallel to the sidewalls. It furthermore is

defined as an average over the plane A (and time t) at height z, parallel to the plates. The z-dependence (p or $\bar{p}$) is different from the x,y-dependence in the A-average (wall or bulk).

To estimate $\epsilon_{\theta,p}$ and $\epsilon_{\theta,\bar{p}}$, recall that $\epsilon_\theta = \kappa\Delta^2 L^{-2} Nu$ and that the heat flux Nu consists of two terms

$$\begin{aligned} Nu &= (\langle u_z\theta\rangle_{A,t}(z) - \kappa\partial_z\langle\theta\rangle_{A,t}(z))/(\kappa\Delta L^{-1}) \\ &= (\epsilon_{\theta,\bar{p}} + \epsilon_{\theta,p})/(\kappa\Delta^2 L^{-2}) = \epsilon_\theta/(\kappa\Delta^2 L^{-2}). \end{aligned} \tag{A 4}$$

Here $\langle ...\rangle_{A,t}$ denotes the average over time and the (x,y)-plane.

For z outside the plate thermal BLs, i.e. for $\epsilon_{\theta,\bar{p}}$, the first term in (A 4) dominates. We estimate $\langle u_z\theta\rangle_{A,t} \sim U\Delta$ and obtain $\epsilon_{\theta,\bar{p}}/(\kappa\Delta^2/L^2) \sim PrRe$. We again emphasize that the thermal dissipation in the sidewall BLs is included in $\epsilon_{\theta,\bar{p}}$ and may even dominate the contributions from the bulk, as the numerical simulations by Verzicco & Camussi (2003) suggest.

For $\epsilon_{\theta,p}$, z is within the plate thermal BLs, i.e. $z/L \approx 0$ or $z/L \approx 1$. Then the second term in (A 4) dominates. Estimating the temperature gradient as Δ/λ_θ gives $\epsilon_{\theta,p}/(\kappa\Delta^2/L^2) \sim L/\lambda_\theta$. To connect the BL width λ_θ with Re, we use the temperature equation $\partial_t\theta = u_j\partial_j\theta + \kappa\partial_j\partial_j\theta$, leading to $Ud^{-1} \sim \kappa\lambda_\theta^{-2}$, which implies $\epsilon_{\theta,p}/(\kappa\Delta^2/L^2) \sim \sqrt{RePr}$. These expressions for $\epsilon_{\theta,p}$ and $\epsilon_{\theta,\bar{p}}$ are given in Grossmann & Lohse (2000). According to this derivation the Reynolds number one has to use in $\epsilon_{\theta,\bar{p}}$ is Re_w, while $\epsilon_{\theta,p}$ is determined by Re_p.

REFERENCES

Ahlers, G. 2000 Effect of sidewall conductance on heat-transport measurements for turbulent Rayleigh–Bénard convection. *Phys. Rev.* E **63**, 015303.

Ahlers, G., Grossmann, S. & Lohse, D. 2002 Hochpräzision im Kochtopf: Neues zur turbulenten Konvektion. *Physik J.* **1** (2), 31–37.

Ahlers, G. & Xu, X. 2001 Prandtl-number dependence of heat transport in turbulent Rayleigh–Bénard convection. *Phys. Rev. Lett.* **86**, 3320–3323.

Blasius, H. 1908 Grenzschichten in Flüssigkeiten bei sehr kleiner Reiburg. *Z. Math. und Phys.* **56**, 1–37.

Castaing, B., Gunaratne, G., Heslot, F., Kadanoff, L., Libchaber, A., Thomae, S., Wu, X. Z., Zaleski, S. & Zanetti, G. 1989 Scaling of hard thermal turbulence in Rayleigh–Bénard convection. *J. Fluid Mech.* **204**, 1–30.

Ching, E. S. C. & Lo, K. F. 2001 Heat transport by fluid flows with prescribed velocity fields. *Phys. Rev.* E **64**, 046302.

Ching, E. S. C. & Pang, K. M. 2002 Dependence of heat transport on the strength and shear rate of circulating flows. *Eur. Phys. J.* B **27**, 559–564.

Ciliberto, S., Cioni S. & Laroche, C. 1996 Large-scale flow properties of turbulent thermal convection. *Phys. Rev.* E **54**, R5901-R5904.

Daya, Z. A. & Ecke, R. E. 2001 Does turbulent convection feel the shape of the container? *Phys. Rev. Lett.* **87**, 184501.

Grossmann, S. & Lohse, D. 2000 Scaling in thermal convection: a unifying view. *J. Fluid. Mech.* **407**, 27–56.

Grossmann, S. & Lohse, D. 2001 Thermal convection for large prandtl number. *Phys. Rev. Lett.* **86**, 3316–3319.

Grossmann, S. & Lohse, D. 2002 Prandtl and Rayleigh number dependence of the Reynolds number in turbulent thermal convection. *Phys. Rev.* E **66**, 016305.

Kadanoff, L. P. 2001 Turbulent heat flow: Structures and scaling. *Phys. Today* **54** (8), 34–39.

Lam, S., Shang, X. D., Zhou, S. Q. & Xia, K. Q. 2002 Prandtl-number dependence of the viscous boundary layer and the Reynolds-number in Rayleigh–Bénard convection. *Phys. Rev.* E **65**, 066306.

Landau, L. D. & Lifshitz, E. M. 1987 *Fluid Mechanics*. Pergamon.

Lui, S. L. & Xia, K.-Q. 1998 Spatial structure of the thermal boundary layer in turbulent convection. *Phys. Rev.* E **57**, 5494–5503.

Niemela, J., Skrbek, L., Sreenivasan, K. R. & Donnelly, R. J. 2001 The wind in confined thermal turbulence. *J. Fluid Mech.* **449**, 169–178.

Niemela, J. & Sreenivasan, K. R. 2003*a* Confined turbulent convection. *J. Fluid Mech.* **481**, 355–384.

Niemela, J. & Sreenivasan, K. R. 2003*b* Rayleigh-number evolution of large-scale coherent motion in turbulent convection. Europhys. Lett. (submitted).

Prandtl, L. 1904 Über Flüssigkeitsbewegung bei sehr kleiner Reibung. *Verhandlungen des III. Int. Math. Kongr., Heidelberg, 1904*. Leipzig: Teubner, pp. 484–491.

Qiu, X. L. & Tong, P. 2001 Large-scale velocity structures in turbulent thermal convection. *Phys. Rev.* E **64**, 036304.

Qiu, X. L. & Xia, K.-Q. 1998*a* Viscous boundary layers at the sidewall of a convection cell. *Phys. Rev.* E **58**, 486–491.

Qiu, X. L. & Xia, K.-Q. 1998*b* Spatial structure of the viscous boundary layer in turbulent convection. *Phys. Rev.* E **58**, 5816–5820.

Siggia, E. D. 1994 High Rayleigh number convection. *Annu. Rev. Fluid Mech.* **26**, 137–168.

Verzicco, R. 2002 Sidewall finite-conductivity effects in confined turbulent thermal convection. *J. Fluid Mech.* **473**, 201–210.

Verzicco, R. & Camussi, R. 1999 Prandtl number effects in convective turbulence. *J. Fluid Mech.* **383**, 55–73.

Verzicco, R. & Camussi, R. 2003 Numerical experiments on strongly turbulent thermal convection in a slender cylindrical cell. *J. Fluid Mech.* **477**, 19–49.

Werne, J. 1993 Structure of hard-turbulent convection in two-dimensions: Numerical evidence. *Phys. Rev.* E **48**, 1020–1035.

Xu, X., Bajaj, K. M. S. & Ahlers, G. 2000 Heat transport in turbulent Rayleigh–Bénard convection. *Phys. Rev. Lett.* **84**, 4357–4360.